Advances in the treatment of the electromagnetic cascade in the TRIPOLI-4® Monte-Carlo code

Davide Mancusi*, Alice Bonin*, François-Xavier Hugot* and Fadhel Malouch*
*Den-Service d'études des réacteurs et de mathématiques appliquées (SERMA),
CEA, Université Paris-Saclay, F-91191, Gif-sur-Yvette, France
Email: davide.mancusi@cea.fr

***Abstract*—TRIPOLI-4® is a Monte-Carlo particle-transport code developed at CEA-Saclay (France) that is employed in the domains of nuclear-reactor physics, criticality-safety, shielding/radiation protection and nuclear instrumentation. The goal of this paper is to report on current developments, validation and verification made in TRIPOLI-4 in the treatment of electron/positron/photon transport. The new capabilities and improvements concern refinements to the electron transport algorithm, the introduction of a charge-deposition score, the new thick-target bremsstrahlung option, the upgrade of the bremsstrahlung model and the improvement of electron angular straggling at low energy. The importance of each of the developments above is illustrated by comparisons with calculations performed with other codes and with experimental data.**

I. Introduction

An accurate description of the electromagnetic cascade is an essential prerequisite for the simulation of the response of a wide range of particle detectors, including in-core and ex-core instrumentation in nuclear reactors. For such applications, one possible simulation tool is provided by the TRIPOLI-4® code [1], a Monte-Carlo particle-transport code developed at CEA-Saclay (France) that is employed in the domains of nuclear-reactor physics, criticality-safety, shielding/radiation protection and nuclear instrumentation. The latest TRIPOLI-4 version (v10) was released in December 2015 and will soon be available to OECD member countries through the NEA Data Bank. This paper reports on some recent developments in TRIPOLI-4 for the simulation of nuclear instrumentation (Section II). Section III compares the predictions of the development version of TRIPOLI-4 with those of TRIPOLI-4 v10 and of other transport codes; additionally, we compare the calculation results against selected experimental data. Conclusions and future plans are discussed in Section IV.

II. Description of the recent developments

We now proceed to describe the new developments in detail.

A. Electron stepping refinement

Electrons (and charged particles in general) exhibit very large cross sections for the interactions with atoms. For this reason, Monte-Carlo codes often resort to a *condensed-history* approach. In this scheme, not all collisions are treated individually, but their effect is represented as a continuous modification of the particle trajectory, which is integrated in small steps. The condensation of elastic-scattering events, in particular, which represent a significant fraction of the total cross section even above the excitation/ionisation thresholds, is handled by *multiple-scattering* formalisms, which are essentially recipes to condense angle-differential distributions for discrete elastic scattering into distributions for the deflection angle along a given path length. As a result of the application of multiple-scattering models, the electron momentum direction is made to deviate from the original direction when the electron moves a certain length (*angular straggling*). Note that, even when using multiple-scattering models, it is customary to single out some collision types for an explicit discrete treatment. In TRIPOLI-4, inelastic collisions leading to secondary electrons above the transport threshold are explicitly handled.

Transport algorithms for charged particles were classified by Berger *et al.* [2]; TRIPOLI-4's algorithm for electrons belongs to Berger's "class I". Electron tracks are assumed to lose a constant fraction α of their kinetic energy along each step, on average. Until TRIPOLI-4 v9, a value of $\alpha = 1 - 2^{-1/8} \simeq 8.3\%$ was assumed. This value was changed to $\alpha = 2\%$ in TRIPOLI-4 v9 on the basis of the results of comparisons with existing experimental data.

The fractional energy loss determines the maximum length ℓ of the step taken by the electron according to

$$\ell = R(T) - R(T \cdot (1-\alpha)) \simeq \frac{\alpha T}{W(T)} + o(\alpha^2), \qquad (1)$$

where $R(T)$ is the continuous slowing-down approximation (CSDA) range for electrons of kinetic energy T and $W(T)$ is the restricted stopping power, which condensates the effect of low-energy bremsstrahlung, elastic scattering and soft inelastic collisions. The actual step taken by the electron may be smaller than the upper limit given by Eq. (1) if the electron undergoes a hard collision (i.e. a collision that was omitted from history condensation) or crosses a geometrical boundary within a shorter distance. In this case, the energy at the step endpoint is adjusted and the direction of the electron is interpolated. In the case of very thin volumes, comparable to or smaller than the maximum step length ℓ, systematic interpolation may sensibly bias the outgoing electron distribution. For this reason, TRIPOLI-4 v10 automatically refines electron transport when approaching geometrical boundaries by dividing the maximum electron step length ℓ by 8.

At low energy, the step length ℓ may become comparable with the precision of TRIPOLI-4's geometry $\varepsilon_{\text{geom}} = 10^{-4}\,\text{cm}$.

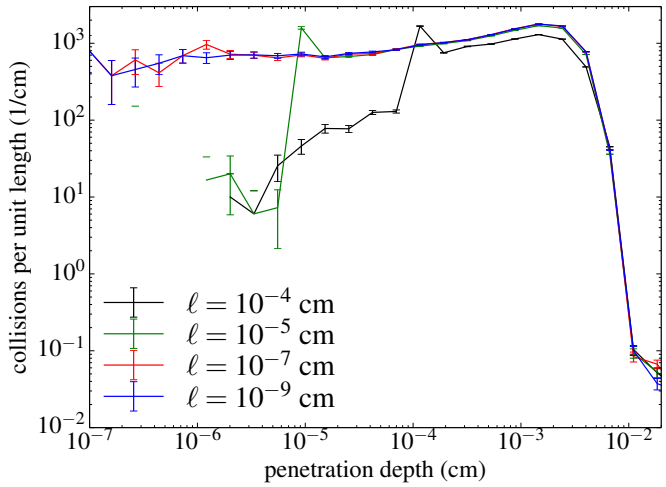

Figure 1. Effect of the minimum forced electron step length ℓ on the space density of collisions, for a 100 keV electron pencil beam impinging perpendicularly on a semi-infinite aluminium slab.

For this reason, it was decided in TRIPOLI-4 v10 that steps shorter than $\varepsilon_{\text{geom}}$ were problematic; attempted steps shorter than $\varepsilon_{\text{geom}}$ were then forcibly extended to $\ell = \varepsilon_{\text{geom}}$. The energy loss of the electron along the extended step was of course accordingly adjusted.

Forcing longer steps, however, leads TRIPOLI-4 to underestimate the number of discrete electron collisions. This happens in particular when the forced step pushes the electron beyond the sampled collision site; in this case (negative residual optical path), the missed collision is neglected and the optical path is resampled.

This behaviour was corrected in the development version of the code. It was observed that there is no practical reason to force steps of length $\varepsilon_{\text{geom}}$ in all cases, but it suffices to do so when the electron is close to a geometrical boundary[1]. The minimum imposed electron step size has therefore been promoted to a user-configurable parameter.

Figure 1 illustrates the effect of the minimum forced electron step size on the collision density generated by a low-energy electron beam in aluminium. The black curve ($\ell = 10^{-4}\,\text{cm}$) can be considered representative of the behaviour of TRIPOLI-4 v10. One can see that the collision density is suppressed at penetration distances smaller than the minimum path length. Additionally, the TRIPOLI-4 v10 default minimum step length of 10^{-4} cm leads to an underestimation of the collision density even well inside the bulk. Depending on the problem, a step length of 10^{-5} cm or smaller must be considered. A value of 10^{-7} cm was found to be suitable for all materials and was used for the following studies.

B. Bremsstrahlung model

The production of bremsstrahlung photons by electrons and positrons in TRIPOLI-4 v10 proceeds according to the specifications of the model described in Berger and Seltzer [3]. However, the same authors presented a newer model for energy-differential cross sections in Seltzer and Berger [4], [5]. Contrary to the 1970 model, the new model is essentially based on the interpolation of tabulated values. The table values are derived from numerical phase-shift calculations for electron energies lower than 2 MeV, and from the analytical high-energy theory above 50 MeV; a numerical interpolation scheme was used to cover the intermediate-energy region. Seltzer and Berger's 1986 model may be considered as the state of the art of the field. It is currently implemented in Geant4 [6], [7] and MCNP6 [8].

We introduced Seltzer and Berger's 1986 model and tables as the new default model for bremsstrahlung in the development version of TRIPOLI-4. A new TRIPOLI-4 keyword was added to control the choice of the bremsstrahlung model.

Figure 2 compares double-differential bremsstrahlung cross sections (for aluminium and uranium targets) calculated with TRIPOLI-4 v10's legacy model [3] (black lines) and the new model [4], [5] (red lines) implemented in the development version. The Geant4 results (green lines) come from an independent implementation of the same model and are shown as a reference. Following Berger and Seltzer [3], the cross sections are multiplied by the factor $\beta^2 k/Z^2$, where β is the relativistic velocity parameter for the electron, k is the photon energy and Z is the nuclear charge.

Clearly, the newly implemented model is in excellent agreement with the Geant4 implementation. One can also notice that the legacy model shows "ripples" at the high-energy ends of the spectra. These seem to be model artefacts and are absent in the new model. Moreover, they only appear when the energy-differential cross section is plotted against the kinetic energy of the *electron* (excitation function) for fixed values of the k/T ratio. It is more common to look at the cross section as a function of k for a given electron kinetic energy T; in this case, the ripple is not apparent.

C. Electron angular straggling at low energy

In TRIPOLI-4, electron angular straggling is described by the Goudsmit-Saunderson model [9]. Specifically, the model describes the probability distribution

$$\frac{\mathrm{d}p}{\mathrm{d}\theta}(\theta; T, \ell),$$

where θ is the deflection angle accumulated along a step of length ℓ by an electron that has kinetic energy T at the beginning of the step. The model relies on the assumption that "sufficiently many" elastic scattering events take place along the considered step. In TRIPOLI-4, this condition is considered to be satisfied for steps longer than

$$\ell_{\text{min,GS}} = 10\lambda_{\text{el}}(T),$$

where $\lambda_{\text{el}}(T)$ is the mean free path for elastic scattering of electrons with kinetic energy T. However, at low energy, the maximum step length proposed by the energy loss criterion (Eq. (1)) may be shorter than the minimum step length

[1]Note that this will necessarily lead to an underestimation of the number of discrete collisions in a very thin layer around geometrical boundaries.

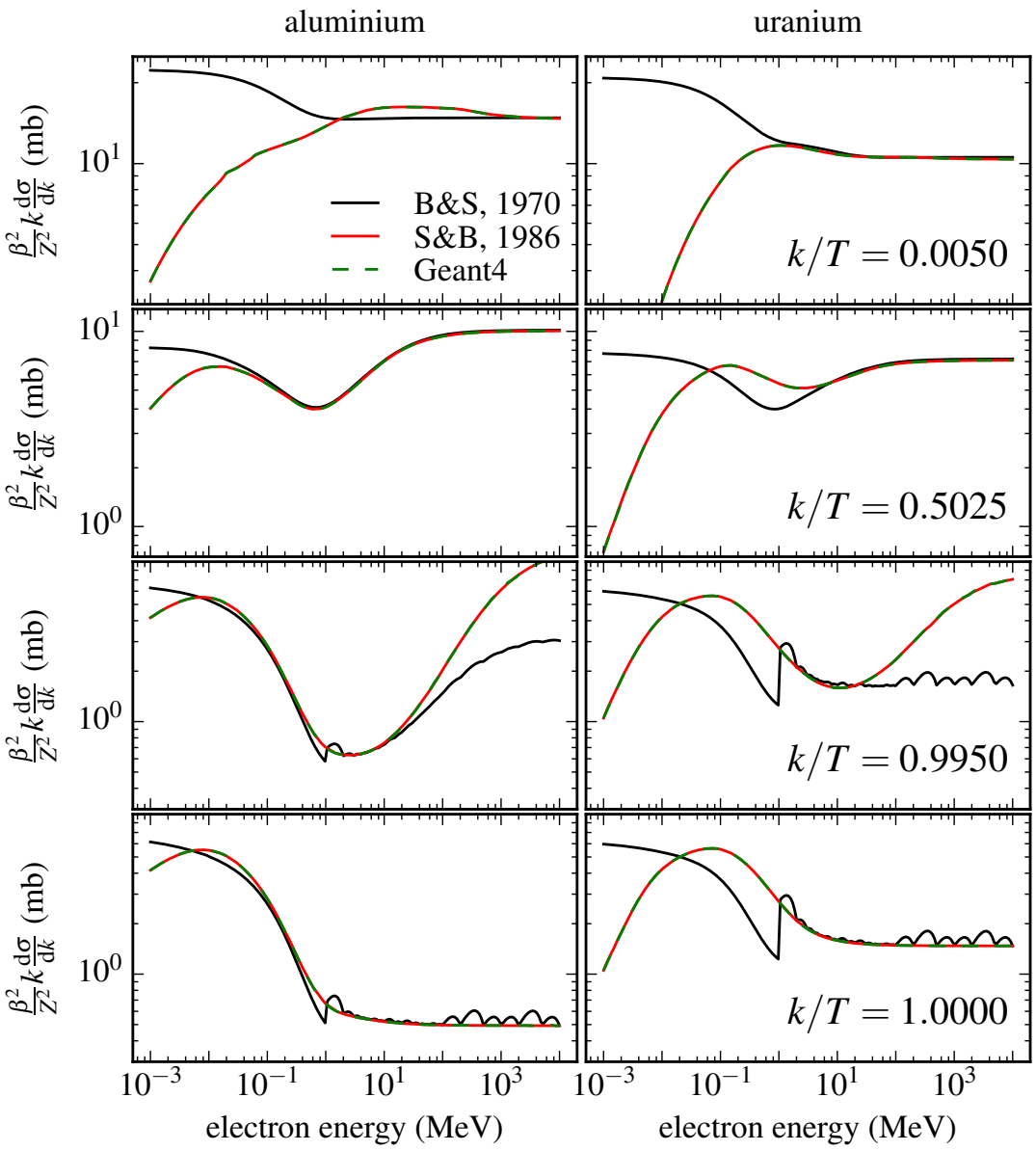

Figure 2. Scaled energy-differential bremsstrahlung cross section for electrons in aluminium (left column) and uranium (right column), plotted against the electron energy, for four fixed values of the ratio of the photon (k) and the electron (T) kinetic energies. The cross sections are rescaled by a suitable factor (see text). We show the results of TRIPOLI-4 v10's legacy model (Berger and Seltzer [3]), the new model (Seltzer and Berger [4], [5]) and Geant4.

required by the Goudsmit-Saunderson model. When these conditions are realised, TRIPOLI-4 v10 does not apply the angular-straggling algorithm; instead, the incident electron is always scattered at right angles with respect to the incident direction, independently on the length of the step. In the development version, we changed the code behaviour to do no scattering when the minimum path-length condition is not met. This modification results in sensibly more forward-peaked electron angular distributions.

Even though both solutions are unphysical, we feel that the latter is more justifiable: indeed, the average scattering cosine for the elastic scattering of a 15 keV electron is $\overline{\cos\theta} \simeq 0.99$ [10]; even 10 such collisions will result in a mean scattering cosine of ~ 0.90. In this sense, doing no multiple scattering is surely a better approximation than always scattering at right angles. Of course, the ideal solution would consist in individually treating elastic collisions below the low-energy validity limit of the Goudsmit-Saunderson model, but this is beyond the scope of this work.

The Goudsmit-Saunderson formalism can in principle be used to condense elastic cross sections from any model/table. In TRIPOLI-4, the cross sections are extracted from different sources depending on the electron energy. Above 256 keV, TRIPOLI-4 uses the Mott cross section [11] with Molière's

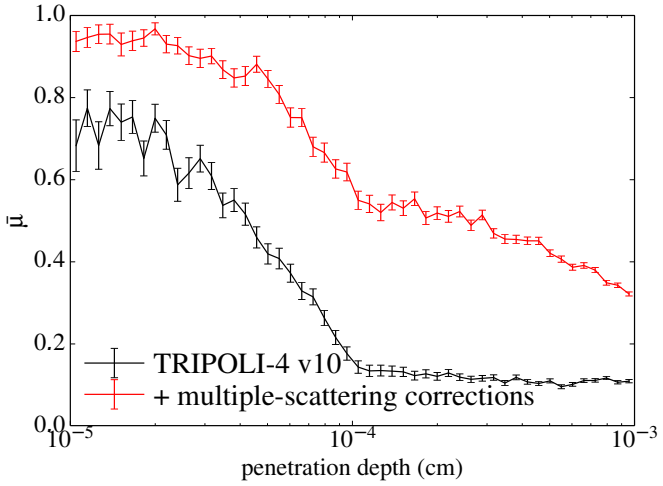

Figure 3. Average direction cosine of the electron momentum along the beam axis, plotted as a function of the penetration depth of a 100 keV electron pencil beam impinging perpendicularly on a semi-infinite aluminium slab. The electron direction is sampled at the collision sites. The different calculations illustrate the effect of the corrections made to angular straggling.

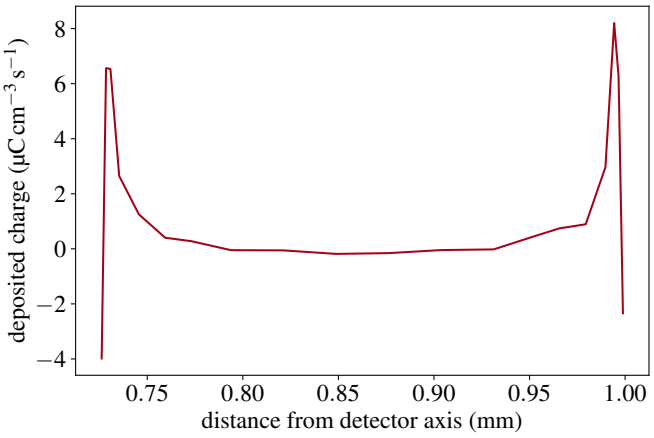

Figure 4. Distribution of charge deposited in the insulator of a self-powered neutron detector exposed to a PWR-like neutron environment, as calculated by TRIPOLI-4 v10.

screening correction [12], [13], as calculated by Feshbach [14] and Sherman [15]. At 256 keV and below, TRIPOLI-4 makes use of data from the Evaluated Electron Data Library (EEDL) [10], which provides integrated and angle-differential large-angle ($\cos\theta < 1 - 10^{-6}$) elastic cross sections. Due to a bug in TRIPOLI-4, the cross sections were incorrectly condensed and angular straggling was overestimated below 256 keV. The correction, which was applied to the development version of the code, results in more forward-peaked angular distributions.

The effect of the modifications in electron multiple scattering are illustrated by Fig. 3, which shows the results of calculations in the same setup considered for Fig. 1, namely a 100 keV electron beam impinging perpendicularly on a semi-infinite slab of aluminium. The plot shows the average direction cosine of the momentum of electrons inducing collisions in the slab, plotted as a function of the penetration depth along the beam axis. One can see that the beam collimation degrades as the electrons penetrate the slab ($\overline{\cos\theta}$ decreases). It is also clear that the corrections made to angular straggling result in sensibly more forward-peaked electron angular distributions. This is consistent with the qualitative comments made above.

D. Charge-deposition score

Self-powered neutron and gamma detectors (SPND and SPGD), often referred to as *collectrons*, are passive devices for in-core measurement of neutron and/or gamma flux. The basic mechanism underlying collectrons is that matter ionized by neutrons or gammas will in general exhibit some degree of spontaneous electrical polarization, which can be detected using appropriate instrumentation. The resulting current, which is ultimately due to electron and positron transport, increases as the radiation field becomes more intense.

In order to characterize the response of a collectron with a Monte-Carlo simulation, it is necessary to calculate the charge-deposition distribution in the instrument. We are aware of at least two ways to do this using Monte-Carlo calculations. The first way consists in calculating all charged-particle currents across the boundary of the detector volume; the net deposited charge can be computed as a signed sum of currents, where incoming currents for negative particles and outgoing currents for positive particles are given a minus sign. This possibility was actually already present in previous versions of TRIPOLI-4, but required manual post-processing of the calculation results.

The alternative estimator, which we have implemented in TRIPOLI-4 version 10, is based on the accumulation of positive and negative increments to the charge deposition every time that a charged particle is born or killed in the considered volume. The two estimators are intimately related by the equation of charge continuity and must yield the same response history by history; however, they may be more or less effective depending on the frequency of the events that trigger score collection (traversal of boundaries in the former case, collisions and absorptions in the latter).

Figure 4 illustrated the new TRIPOLI-4 capability by presenting the result of a calculation of the distribution of charge deposited in the insulator of a collectron. The particle source for this calculation is an in-core neutron environment for a generic pressurized-water nuclear reactor. Note that this distribution is only one of the building blocks that are necessary for the simulation of the collectron response. The full simulation of the detector current also requires a physical model for the electrostatic response of the device, and thus cannot be carried out by radiation-transport codes alone.

E. Thick-target bremsstrahlung mode

The full simulation of the electromagnetic cascade, including electron and positron transport, is very CPU intensive when compared to a pure photon simulation. However, pure photon transport does not take into account bremsstrahlung

photons emitted by secondary electrons; when the photon energy is sufficiently high (say above 1 MeV), pure photon transport will underestimate the secondary photon flux. In cases where a rough estimation of the secondary bremsstrahlung flux is sufficient, it is advantageous to consider a simplified calculation mode (*thick-target bremsstrahlung*, TTB) where electron production and transport are directly replaced by the emission of secondary bremsstrahlung photons; this effectively amounts to replacing secondary electron production with a photon-photon scattering vertex. Since the additional secondary photons are emitted from the starting point of the suppressed electron track, the approximation is generally understood to be less severe in thick volumes, hence its name. A similar approximation exists in MCNP6 [8]. Contrary to TRIPOLI-4, MCNP6's TTB model is activated by default in pure photon calculations.

The TRIPOLI-4 TTB implementation proceeds along the lines indicated by Kitsos, Diop, Assad, *et al.* [16] and Riz [17]. The most notable difference with respect to the MCNP6 implementation concerns the fact that TRIPOLI-4 accounts for the angular straggling of the condensed electrons; therefore, the bremsstrahlung photons are not necessarily emitted around the initial electron direction. Additionally, the TRIPOLI-4 TTB implementation also allows the use of electron sources; in this case, only tertiary electrons generated by secondary photons are replaced with the corresponding bremsstrahlung photons.

As an illustration, we consider the transmission of 20 MeV photons through a 10 cm-thick lead slab. The point-like photon source is located at 3.3 m from the face of the lead slab and is assumed to emit photons uniformly within a 4° (full aperture) cone directed towards the slab. We score the photon flux over a rough 8-group grid within a box located on the opposite side of the lead slab. The detector size is such that it covers roughly 1/4 of the solid angle spanned by the unscattered beam.

Figure 5 shows the TRIPOLI-4 calculation results obtained with electron-positron-photon transport ("full"), with the thick-target-bremsstrahlung approximation ("TTB") and with photon transport only ("photon"). If we take the full TRIPOLI-4 calculation as a reference, we can observe that a pure photon TRIPOLI-4 calculation severely underestimates the photon flux below 15 MeV. This is an indication of the fact that the contribution of secondary electron bremsstrahlung is large. The full TRIPOLI-4 and MCNP6 calculations are in good agreement. The TRIPOLI-4 TTB calculation remains within 30 % of the reference calculation, but the CPU time is reduced by about a factor of 10. Note that the MCNP6 TTB calculation is much less accurate for this test case: the photon flux at the lowest energies is overestimated by about a factor of 10. This is mostly due to the fact that, as far as we understand, MCNP6 neglects angular straggling of the suppressed secondary electrons. In TRIPOLI-4, the net effect of angular straggling is to diffuse the forward-peaked bremsstrahlung photons towards larger angles; a larger fraction of the transmitted photons may therefore miss the detector. Since this does not happen in MCNP6, too many photons are emitted in the forward direction, overestimating the score. The importance of angular straggling is illustrated by the cyan curve of Fig. 5, which was obtained by suppressing electron angular straggling in TRIPOLI-4.

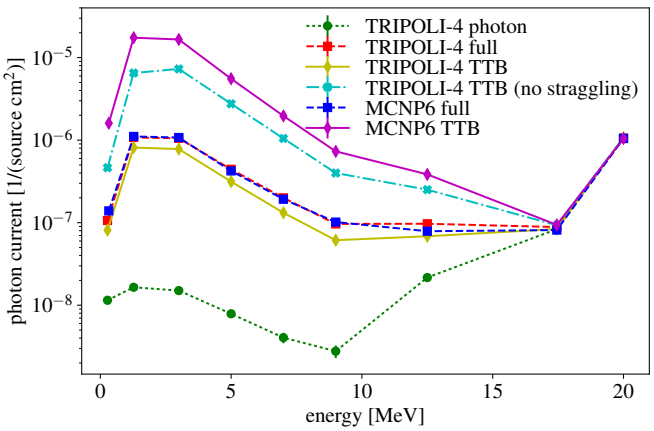

Figure 5. Energy spectrum of photons transmitted through a thick lead slab, as calculated by TRIPOLI-4 and MCNP6, with and without thick-target bremsstrahlung approximation. An additional TRIPOLI-4 calculation with thick-target bremsstrahlung but without electron angular straggling is also presented. Statistical errors on the calculated spectra are too small to be visible.

III. Verification and validation

We now turn to the verification and validation (V&V) of the new developments for low-energy electrons (Sec. II). We shall consider two types of observables

- Electron transmission/reflection coefficients. These observables are expected to be sensitive to angular straggling.
- Thick-target bremsstrahlung spectra. These observables represent the energy and/or angular distributions of photons generated by the impact of electron beams with thick targets. Obviously, these observables probe the bremsstrahlung process which is responsible for the photon emission. It is perhaps less evident that they are also quite sensitive to the angular straggling of the primary electrons. The reason is that the bremsstrahlung angular distribution is sensibly forward-peaked, even at low energies. Therefore, the angular distribution of the emitted photons also reflects the angular distribution of the braking electrons.

A. Electron transmission and reflection

Inspired by Seltzer and Berger [18] and Kadri, Ivanchenko, Gharbi, *et al.* [19], we present calculations of transmission, reflection and absorption coefficients of electron beams in thin foils. The number transmission (T_N) and reflection coefficients (R_N) respectively represent the average number of transmitted (reflected) electrons per incident electron. The energy transmission (T_E) and reflection coefficients (R_E) respectively represent the fraction of the beam energy that is transmitted

Table I
TRANSMISSION, REFLECTION AND ABSORPTION COEFFICIENTS FOR 100 keV ELECTRONS THROUGH 25.4 µm-THICK ALUMINIUM AND TITANIUM FOILS, EXPRESSED IN PERCENTAGE POINTS. CALCULATIONS WERE PERFORMED WITH TRIPOLI-4 v10 AND TRIPOLI-4 (DEVELOPMENT VERSION); THE GEANT4 VALUES ARE TAKEN FROM KADRI, IVANCHENKO, GHARBI, *et al.* [19]. THE STATISTICAL UNCERTAINTIES ON THE TRIPOLI-4 VALUES ARE SMALLER THAN THE LAST REPORTED SIGNIFICANT DIGIT. SEE TEXT FOR THE DEFINITION OF THE COEFFICIENTS.

		TRIPOLI-4 v10 (%)	TRIPOLI-4 dev (%)	Geant4 (%)
Al	T_N	18.2	65.4	60.7
	R_N	64.7	9.0	12.6
	T_E	6.7	42.4	40.3
	R_E	43.2	4.5	7.2
	ϕ_A	50.2	53.1	53.2
Ti	T_N	11.7	10.1	8.2
	R_N	67.8	17.8	18.6
	T_E	3.2	4.0	3.9
	R_E	47.6	9.7	11.8
	ϕ_A	49.2	86.4	84.7

through (reflected by) the foil. By difference, one can also define the energy absorption coefficient $\phi_A = 1 - T_E - R_E$.

In this work, we concentrate on transmission and reflection of 100 keV electrons through 1 mil-thick aluminium and titanium targets ($1\,\text{mil} = 10^{-3}\,\text{in} = 25.4\,\mu\text{m}$). Table I compares the results of calculations performed with TRIPOLI-4 v10 and with the development version of TRIPOLI-4. Geant4 calculation results from the literature [19] are also included for comparison; note that these results were produced to illustrate Geant4's implementation of the Goudsmit-Saunderson model, which is not Geant4's default angular-straggling model [20].

The first observation is that the TRIPOLI-4 v10 results show little sensitivity to the target. This is probably connected to the underestimation of the mean free path for elastic scattering (Sec. II-C): indeed, an overestimated elastic cross section leads to excess multiple scattering. If electrons scatter too much and at too large angles, electron transport becomes akin to diffusion; under these conditions, one would expect the transmission and reflection coefficients to be essentially dominated by the geometry, which is the same in both cases (same thickness). Comparison with the other calculations makes it quite clear that this picture is largely erroneous.

The recent TRIPOLI-4 developments bring a substantial improvement. The new results are qualitatively similar to the Geant4 calculations. As a general trend, in the comparison with Geant4, TRIPOLI-4 seems to yield smaller reflection and larger transmission coefficients. This is shown in Table I for the aluminium target, but actually holds for other targets, too. These facts may probably be explained by considering that Geant4 singles out large-angle elastic scattering as a separate process[2]. Backward elastic-scattering events, especially those

[2]Geant4's electron-transport algorithm falls in class II of Berger *et al.*'s ([2]) classification.

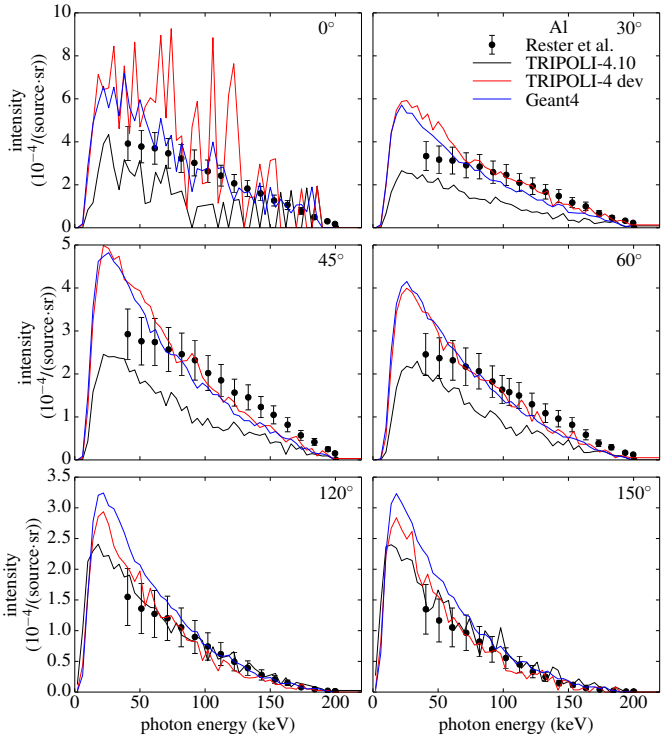

Figure 6. Double-differential photon intensity spectra at various degrees for 200 keV electrons on a 69 mg/cm^2 aluminium target, as measured by Rester, Dance and Derrickson [21] and as calculated by TRIPOLI-4 v10, TRIPOLI-4 development version and Geant4 v10.2p1. The large fluctuations in the calculations at 0° are statistical artefacts due to insufficient sampling. The calculation affected by the largest statistical uncertainties is TRIPOLI-4 development version; for all angles except 0°, the uncertainties are of the order of 4 % to 8 % at 50 keV, 10 % at 100 keV and 40 % at 150 keV.

that take place at small penetration depths, are expected to yield a sizeable contribution to reflection. It is clear that the effect of these collisions cannot be accurately modelled in the framework of an angular-straggling model, which by definition aims at capturing the mean effect of a large number of soft collisions.

B. Bremsstrahlung spectra from thick targets

We now turn to the study of the emission of bremsstrahlung photons from thick (e.g. stopping) targets. We consider two experiments in which double-differential photon spectra were measured from bremsstrahlung conversion of an electron beam.

1) Rester, Dance and Derrickson [21]: In the first experiment [21], photon spectra were measured from 0° to 150° for beryllium, aluminium, iron, tin and gold targets. The lowest beam energy was 200 keV. The target was placed at right angles with respect to the electron beam direction, which results in an azimuthally symmetric angular distribution and in an unambiguous definition of the detector position.

For conciseness, we limit our presentation to the aluminium and tin targets at 200 keV. Figures 6 and 7 compare the measured double-differential intensity spectra with several calculations. Clearly, the new developments improve the perfor-

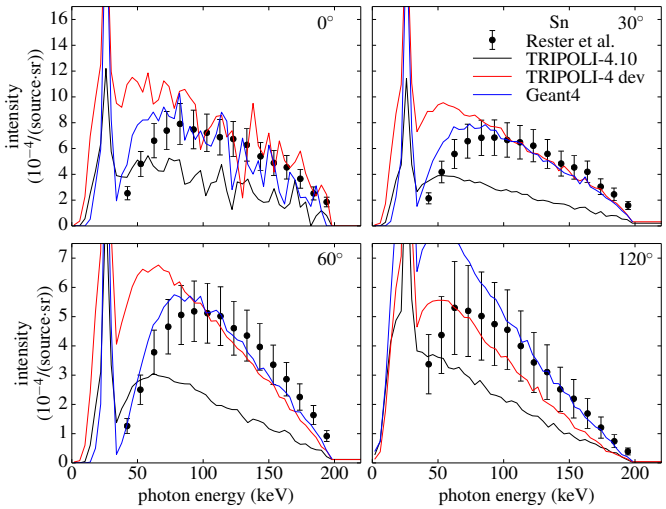

Figure 7. Same as Fig. 6, but for an 82 mg/cm^2 tin target.

mance of TRIPOLI-4 for this dataset. We have verified that the most relevant contributions come from the new bremsstrahlung model.

The development version of TRIPOLI-4 is in excellent agreement with all the experimental data for the aluminium target, and with the experimental data above 100 keV for the tin target. Geant4 calculations, shown for comparison, are generally in slightly less good agreement with the experimental data, with the notable exception of the low-energy portions of the tin spectra. The fall-off of the tin spectra between 40 keV to 70 keV in Geant4 is likely due to secondary photon absorption. At this stage, it is difficult to determine why TRIPOLI-4 does not show the same pattern. A comparison of the elementary photon cross sections in tin between TRIPOLI-4 and Geant4 will help clarify whether the discrepancy between the codes reflects differences in photon transport or in the distributions of the produced photons.

2) Faddegon, Ross and Rogers [22]: We also present the results of calculations for the high-energy thick-target bremsstrahlung benchmark experiments by Faddegon, Ross and Rogers [22]. The electron beam energy for this experiment was 15 MeV. We modelled the experimental geometry with TRIPOLI-4 and MCNP6, including the titanium exit window, the silicon beam monitor and the steel window (for angles between 0° and 10°). We tallied the double-differential photon yield in scoring regions with 1° acceptance at 3 m from the target; in other words, the detector was not modelled in detail.

For the sake of conciseness, we limit our presentation to the results for the lead target, which are representative of the general agreement between the codes and the experimental data. Figure 8 shows the double-differential photon yield calculated by MCNP6, TRIPOLI-4 v10 and TRIPOLI-4 development version. The two TRIPOLI-4 versions yield very similar results for this benchmark. The average difference between the two code versions is of the order of a few percent; the maximum discrepancy appears at the high-energy end of the 2° and

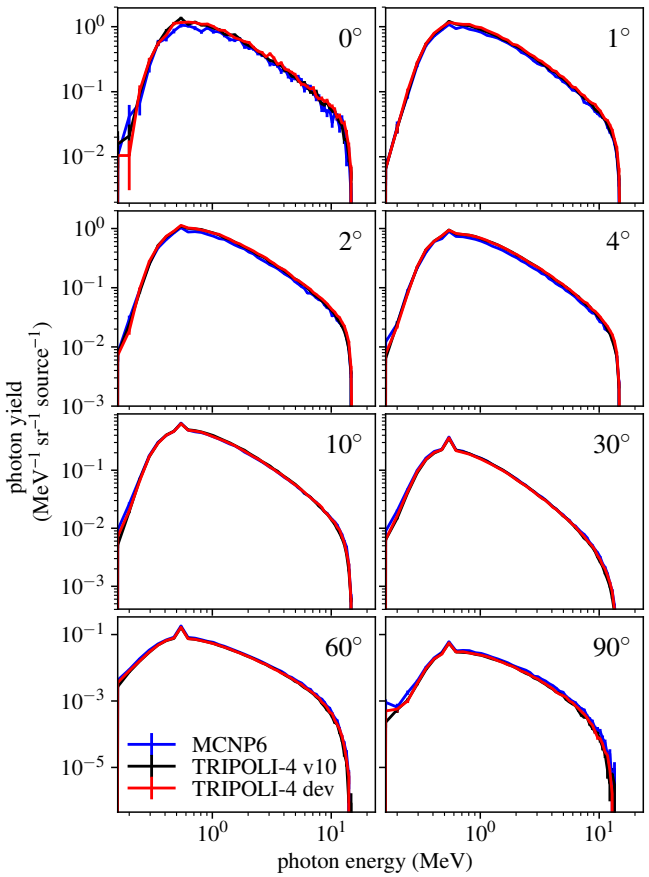

Figure 8. Double-differential energy-angle photon yields for the Faddegon, Ross and Rogers [22] benchmark, as calculated by MCNP6, TRIPOLI-4 v10 and TRIPOLI-4 development version.

4° spectra and is of the order of 10 %. These relatively small variations contrast with the results of Section III-A and illustrate the fact that the new TRIPOLI-4 developments are mostly relevant for low-energy electron transport. The comparison with MCNP6 shows discrepancies of the order of 10 %. In all cases, the discrepancies among TRIPOLI-4 v10, TRIPOLI-4 development version and MCNP6 are of the same order of magnitude of the statistical uncertainty on the calculated spectra.

Figure 9 shows the angular distribution of the photon yield integrated over energies larger than the experimental detection threshold. Again, we see that TRIPOLI-4 v10 and TRIPOLI-4 development version are in good agreement with each other; the difference between TRIPOLI-4 and MCNP6 is of the order of 10 %, with TRIPOLI-4 being generally slightly closer to the experimental data than MCNP6.

IV. Conclusions

We have presented the new TRIPOLI-4 developments concerning the treatment of the electromagnetic cascade, namely:

- the refinement of the electron stepping algorithm;
- the implementation of a new model for the energy-differential bremsstrahlung cross section;

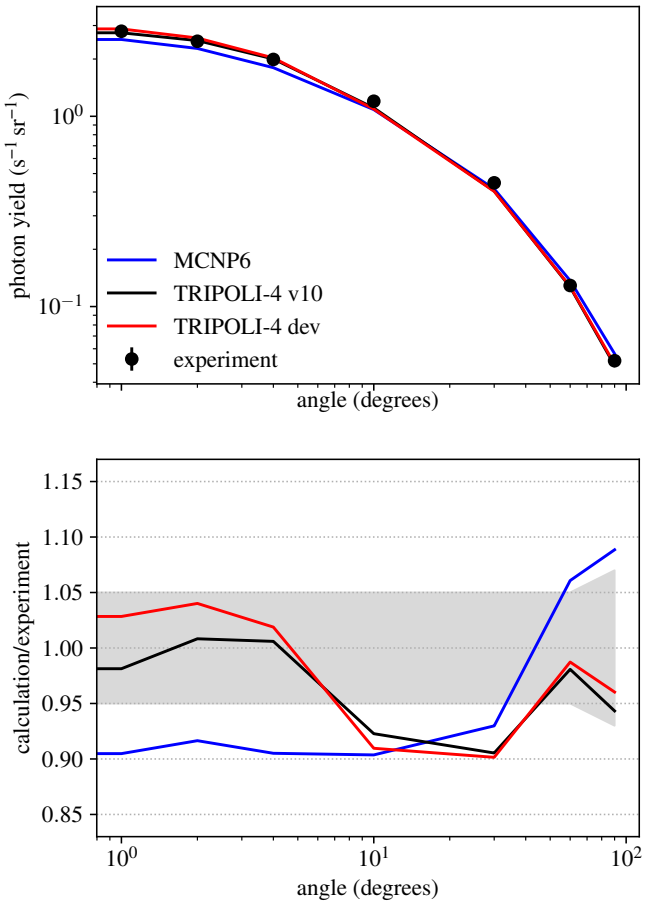

Figure 9. Top: angular distribution for the integrated photon flux over energies larger than the experimental detection threshold, as measured by Faddegon, Ross and Rogers [22] and as calculated by MCNP6, TRIPOLI-4 v10 and TRIPOLI-4 development version. Bottom: ratio of calculations to the experimental data; the shaded region represents the experimental uncertainty. The statistical uncertainties on the Monte-Carlo calculations are negligible with respect to the experimental uncertainties.

- a more careful treatment of the condensation of electron elastic cross sections into angular-straggling distributions;
- the implementation of a charge-deposition score;
- the introduction of the thick-target-bremsstrahlung simplified calculation mode.

The impact of these developments is highlighted by the comparison of TRIPOLI-4 calculation results with experimental data and with the results of other transport codes. The new developments improve the agreement with the experimental data in all cases, sometimes in a major way. The experimental datasets considered in this report have been integrated into TRIPOLI-4's V&V test suite.

Analysis of the remaining discrepancies with the experimental data suggests the way for future developments. Electron transmission and (especially) reflection coefficients may be improved by implementing a hybrid continuous-discrete transport scheme, where hard elastic electron collisions ("hard" in a sense to be defined, e.g. large-angle collisions, or giving rise to large energy losses) are not condensed into multiple scattering and are explicitly singled out. Additionally, it is perhaps worth investigating the reason for the discrepancy between TRIPOLI-4, on one side, and Geant4 and the experimental data, on the other side, in the calculation of photon spectra from thick-target electron bremsstrahlung in tin (Sec. III-B1). This shortcoming may be related to differences in low-energy photon absorption.

Finally, we plan to conduct further verification and validation for the newly-developed score for charge deposition and the simplified thick-target-bremsstrahlung calculation mode.

Acknowledgment

TRIPOLI-4® is a registered trademark of CEA. Partial financial support from EDF (Électricité de France) is gratefully acknowledged.

References

[1] E. Brun, F. Damian, C. M. Diop, E. Dumonteil, F.-X. Hugot, C. Jouanne, Y. K. Lee, F. Malvagi, A. Mazzolo, O. Petit, J. Trama, T. Visonneau and A. Zoia, "TRIPOLI-4®, CEA, EDF and AREVA reference Monte Carlo code", *Ann. Nucl. Energy*, vol. 82, pp. 151–160, Aug. 2015. DOI: 10.1016/j.anucene.2014.07.053.

[2] M. J. Berger *et al.*, "Monte Carlo calculation of the penetration and diffusion of fast charged particles", *Meth. Comp. Phys.*, vol. 1, pp. 135–215, 1963.

[3] M. J. Berger and S. M. Seltzer, "Bremsstrahlung and photoneutrons from thick tungsten and tantalum targets", *Phys. Rev. C*, vol. 2, pp. 621–631, 2 Aug. 1970. DOI: 10.1103/PhysRevC.2.621.

[4] S. M. Seltzer and M. J. Berger, "Bremsstrahlung spectra from electron interactions with screened atomic nuclei and orbital electrons", *Nucl. Instrum. Meth. B*, vol. 12, no. 1, pp. 95–134, 1985.

[5] ——, "Bremsstrahlung energy spectra from electrons with kinetic energy 1 keV–10 GeV incident on screened nuclei and orbital electrons of neutral atoms with $Z = 1$–100", *At. Data Nucl. Data Tables*, vol. 35, no. 3, pp. 345–418, 1986. DOI: 10.1016/0092-640X(86)90014-8.

[6] J. Allison, K. Amako, J. Apostolakis, *et al.*, "Recent developments in Geant4", *Nucl. Instrum. Meth. Phys. Res. Sect. A*, vol. 835, pp. 186–225, 2016. DOI: 10.1016/j.nima.2016.06.125.

[7] *Geant4 Physics Reference Manual*, version 10.2, Geant4 collaboration, Dec. 2015. [Online]. Available: http://geant4.web.cern.ch/geant4/UserDocumentation/UsersGuides/PhysicsReferenceManual/BackupVersions/V10.2/fo/PhysicsReferenceManual.pdf.

[8] T. Goorley, M. James, T. Booth, *et al.*, "Initial MCNP6 release overview", *Nucl. Technol.*, vol. 180, no. 3, pp. 298–315, Dec. 2012.

[9] S. Goudsmit and J. L. Saunderson, "Multiple scattering of electrons", *Phys. Rev.*, vol. 57, pp. 24–29, 1 Jan. 1940. DOI: 10.1103/PhysRev.57.24.

[10] S. T. Perkins, D. E. Cullen and S. M. Seltzer, "Tables and graphs of electron-interaction cross sections from 10 eV to 100 GeV derived from the LLNL Evaluated Electron Data Library (EEDL), $Z = 1$–100", Lawrence Livermore National Laboratory, Tech. Rep. UCRL-50400, Nov. 1991.

[11] N. F. Mott, "The scattering of fast electrons by atomic nuclei", *P. R. Soc. Ac*, vol. 124, no. 794, pp. 425–442, 1929. DOI: 10.1098/rspa.1929.0127.

[12] G. Molière, "Theorie der Streuung schneller geladener Teilchen i: Einzelstreuung am abgeschirmten Coulomb-Feld", *Z. Naturforsch.*, vol. 2, no. a, pp. 133–145, 1947.

[13] ——, "Theorie der Streuung schneller geladener Teilchen ii: Mehrfach- und Vielfachstreuung", *Z. Naturforsch.*, vol. 3, no. a, pp. 78–97, 1948.

[14] H. Feshbach, "The Coulomb scattering of relativistic electrons and positrons by nuclei", *Phys. Rev.*, vol. 88, pp. 295–297, 2 Oct. 1952. DOI: 10.1103/PhysRev.88.295.

[15] N. Sherman, "Coulomb scattering of relativistic electrons by point nuclei", *Phys. Rev.*, vol. 103, pp. 1601–1607, 6 Sep. 1956. DOI: 10.1103/PhysRev.103.1601.

[16] S. Kitsos, C. M. Diop, A. Assad, J. C. Nimal and P. Ridoux, "Improvement of gamma-ray S_n transport calculations including coherent and incoherent scatterings and secondary sources of bremsstrahlung and fluorescence: Determination of gamma-ray buildup factors", *Nucl. Sci. Eng.*, vol. 123, no. 2, pp. 215–227, 1996.

[17] D. Riz, "Calculation and use of multigroup cross sections including electron-photon cascade for a 3D Monte Carlo neutron-gamma transport code. Comparisons with MCNP-4B", in *Proceedings to the 2000 ANS International Topical Meeting on Advances in Reactor Physics and Mathematics and Computation into the Next Millennium (PHYSOR-2000)*, Pittsburgh, PA, USA, May 2000.

[18] S. M. Seltzer and M. J. Berger, "Transmission and reflection of electrons by foils", *Nucl. Instrum. Meth.*, vol. 119, pp. 157–176, 1974. DOI: 10.1016/0029-554X(74)90747-2.

[19] O. Kadri, V. Ivanchenko, F. Gharbi and A. Trabelsi, "Incorporation of the Goudsmit–Saunderson electron transport theory in the Geant4 Monte Carlo code", *Nucl. Instrum. Meth. B*, vol. 267, no. 23–24, pp. 3624–3632, 2009. DOI: 10.1016/j.nimb.2009.09.015.

[20] V. N. Ivanchenko, O. Kadri, M. Maire and L. Urban, "Geant4 models for simulation of multiple scattering", *J. Phys.: Conf. Ser.*, vol. 219, no. 3, p. 032 045, 2010.

[21] D. H. Rester, W. E. Dance and J. H. Derrickson, "Thick target bremsstrahlung produced by electron bombardment of targets of Be, Sn, and Au in the energy range 0.2–2.8 MeV", *J. Appl. Phys.*, vol. 41, no. 6, pp. 2682–2692, 1970. DOI: 10.1063/1.1659282.

[22] B. A. Faddegon, C. K. Ross and D. W. O. Rogers, "Angular distribution of bremsstrahlung from 15-MeV electrons incident on thick targets of Be, Al, and Pb", *Med. Phys.*, vol. 18, no. 4, pp. 727–739, 1991. DOI: 10.1118/1.596667.